Electronic Supplementary Material (ESI) for RSC Advances.

Supplementary Information

Another possibility for peak broadening in the cyclic voltammograms exhibited in figure 1 could be ascribed to slow electrolyte diffusion through the film. This aspect was studied using hexacyanoferrate (II) as a probe, with the results shown in Figure S1. No significant differences could be observed in the area, middle potential and line shape of the Faradaic peaks for the films with 5 bilayers of (HPW/PAH) on (PDMS/PAH) or just PAH. It turns out that the films are porous enough to prevent any diffusional barrier to the charged species during the electrochemical process, and this alternative interpretation can be ruled out.

Figure S1. Cyclic Voltammograms in an aqueous solution 6.0 10^{-3} mol L^{-1} of $K_3Fe(CN)_6$ in 0.10 mol L^{-1} of $NaClO_4$ at pH=1.0 (in $HClO_4$ medium) for a bare ITO substrate and pre-coated ITO substrates with PAH or (PDMS/PAH) followed by deposition of 5-bilayers of (HPW/PAH). Scan rate: 10 mV s^{-1}.

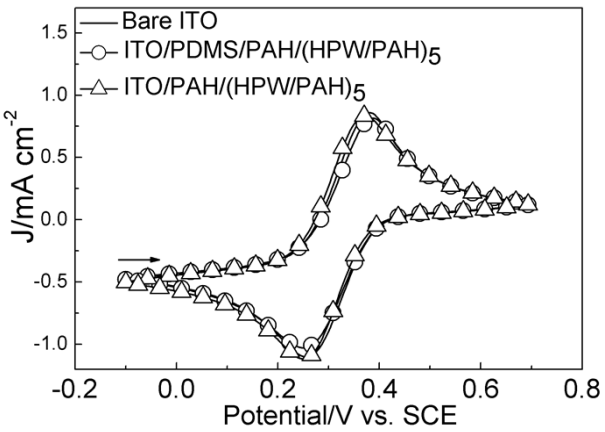

Figure S2. Cyclic Voltammograms for various potential sweeps for 5 bilayers of (HPW/PAH) on ITO pre-coated with (A) APTS and (B) Chitosan. The supporting electrolyte was an aqueous solution of $HClO_4$ at pH=1.0. Scan rate: 20 mV s^{-1}.

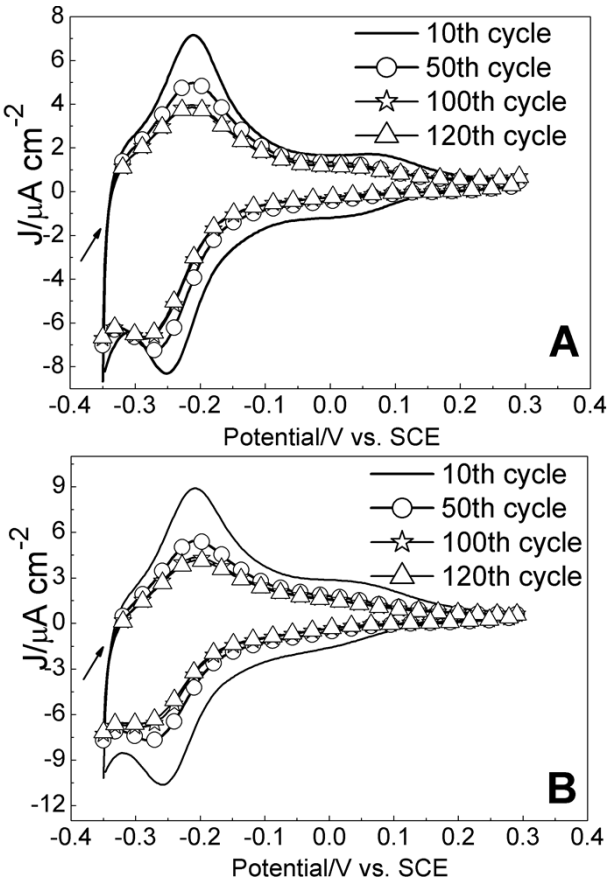

Figure S3 shows the FT-IRRA spectra for PDMS grown on an oxidized Ge single crystal (GeO_x/Ge(111)) taken with a p-polarized IR beam for various adsorption times, which display the typical bands at 1259 cm^{-1} assigned to the symmetric deformation, δ_{sym} Si-CH_3, of the lateral group of PDMS. The bands at 1023 cm^{-1} and 1087 cm^{-1} are ascribed to asymmetric Si-O-Si stretchings. In subsidiary experiments, the spectra were found to be weakly affected when s-polarized light was used (results not shown), the observed weak changes being consistent with an adsorption of PDMS with no preferential orientation [1]. The FT-IRRAS technique was also used to investigate the kinetics of adsorption for the PDMS coating layer, monitoring the area of the Si-CH_3 band as a function of time. The inset in S3 shows that a full PDMS layer was formed within 185 s only for a GeO_x/Ge(111) substrate.

Figure S4A shows the FT-IRRA spectrum for PDMS on GeO_x/Ge while Figure S4B shows the spectrum for PAH adsorbed on PDMS/GeO_x/Ge. Gaussian components for the bands of the spectra are represented by broken lines. The δ_{sym} Si-CH_3 band at 1259 cm^{-1} appears in both spectra, which is evidence for the presence of PDMS. However, its intensity and integrated area are lower for the (PDMS/PAH) film, which may be attributed to two reasons. i) an irreversible desorption of PDMS when PAH is adsorbed; ii) PDMS molecules diffusion to the solution-film interface, followed by redeposition atop the PAH layer. The second hypothesis is found consistent when the attenuated total reflection process is analyzed. Upon reaching the reflecting surface, part of the incident infrared creates an evanescent electric field (evanescent wave). The

detected radiation intensity depends on the attenuation suffered by the incident infrared radiation as the material probed is more distant from the Ge surface. The expression for the evanescent wave penetration depth (d_p) for infrared irradiation is [2]:

$$d_p = \left(\frac{\lambda}{2\pi \left[n_1^2 \sin^2 \theta - {n_2}^2 \right]^{1/2}} \right) \qquad (1)$$

where λ is the wavelength, n_1 is the refractive index of Ge (4.0 for this infrared region), n_2 is the refractive index of the medium (1.410 for the PDMS used) and θ = 45^o is the angle of incidence. With these parameters, the maximum penetration of the evanescent wave is 515 nm for the Si-CH_3 band at 1259 cm^{-1}. Since the effective sensing depth is given by $d_p/2$ [3], the signal for a material located ca. 200 nm from the Ge interface dramatically decreases. Hence, the second hypothesis, according to which PDMS molecules diffuse to the solution-film interface, is a more likely explanation for the data in Figure S4.

Figure S3. FT-IRRA spectra obtained in p-polarization for different adsorption times of PDMS a GeO_x/Ge(111) substrate. The inset shows the area of the band ascribed to Si-CH_3 band at 1259 cm^{-1} versus adsorption time.

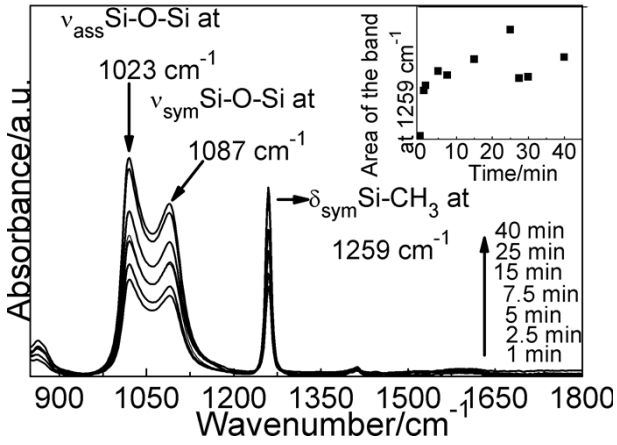

Figure S4. FT-IRRA spectra for GeOx/Ge(111) substrates for (A) PDMS and B) PAH adsorbed on PDMS. The black curves represent the experimental data and are superimposed on the fitted spectra. The broken lines represent the Gaussian components of the absorption bands.

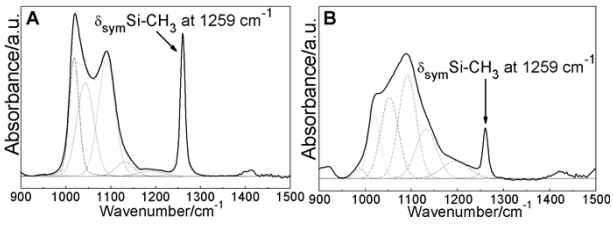

Figure S5. SPR signal for the adsorption of PAH and HPW layers on a disk of polycrystalline gold that had been previously coated ex-situ with PDMS.

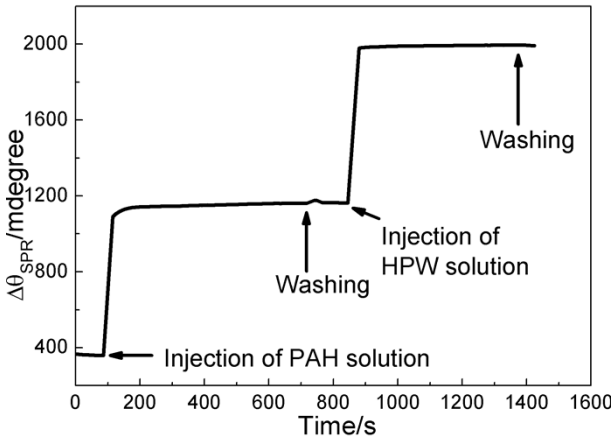

Figure S6. AFM images in the contact mode obtained with a silicon nitride tip for: (A) ITO coated with a PDMS layer deposited during 30 min from an isopropyl alcohol solution at T=298 K and (B) bare ITO.

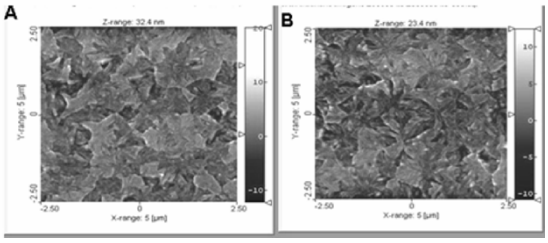

Figure S7. FEG-SEM images for modified ITO substrates with 5-bilayers (HPW/PAH) as prepared when ITO is pre-coated with (A) (PDMS/PAH) (B) PAH.

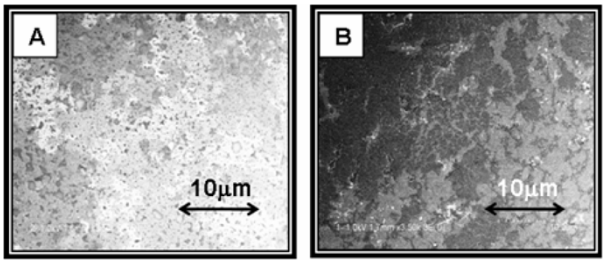

Figure S8. Wide-scan XP spectra for 5-bilayers (HPW/PAH) LbL film prepared on ITO substrates pre-coated with PAH (A) and (PDMS/PAH) (B). The arrows identify the corresponding elements in the samples.

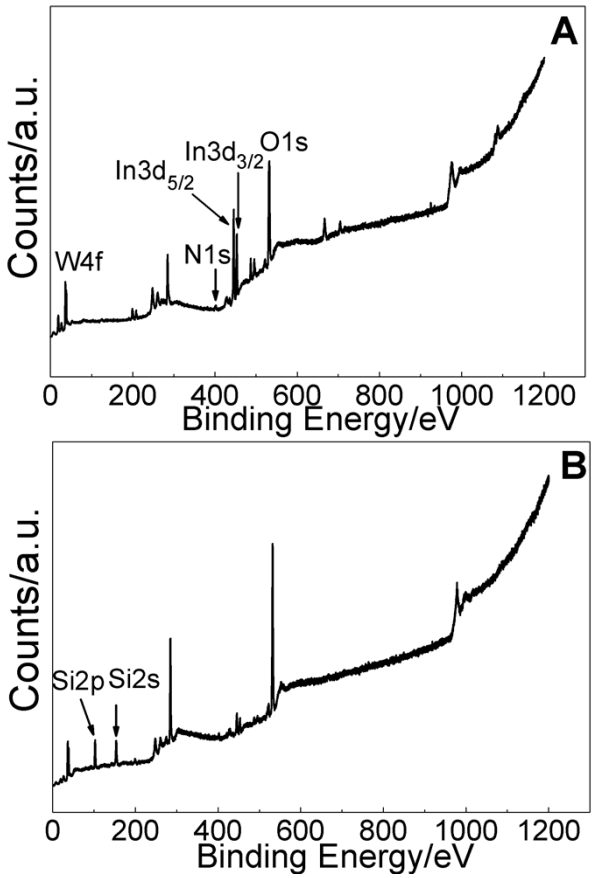

Figure S9: High resolution XP spectra for ITO modified with 5 bilayers of (HPW/PAH) pre coated with PAH. W $4f_{7/2}$ region for as prepared film (A), W $4f_{7/2}$ region after potential cycling (B), N 1s region for as prepared film (C), N 1s region after potential cycling (D).

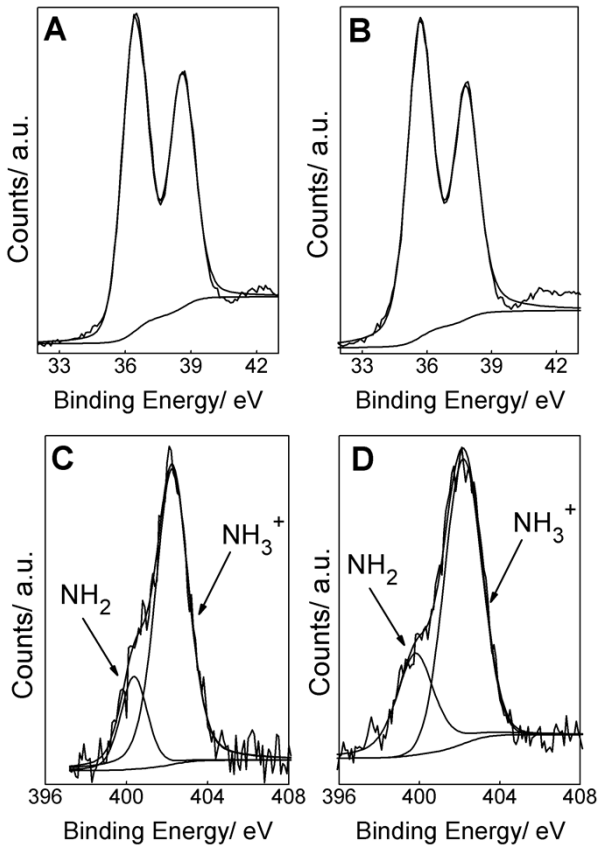

Figure S10. Cyclic Voltammograms for bare ITO electrode in the absence (solid line) and in the presence of 3.0 10^{-7} mol L^{-1} of melamine and of 5.0 10^{-6} mol L^{-1} atrazine. The supporting electrolyte was an aqueous solution of $HClO_4$ at pH=1.0. Scan rate: 20 mV s^{-1}.

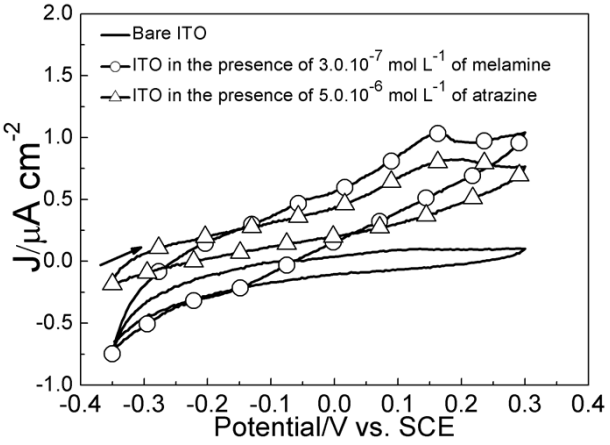

Figure S11: Differential pulse voltammograms in the anodic region for a 5-bilayers (HPW/PAH) LbL film on ITO substrate pre-coated with (PDMS/PAH) at different melamine concentrations varying from 4.0 10^{-8} mol L^{-1} to 1.0 10^{-7} mol L^{-1}. The inset shows the anodic current density as a function of the melamine concentration. The supporting electrolyte was an aqueous solution of $HClO_4$ at pH=1.0.

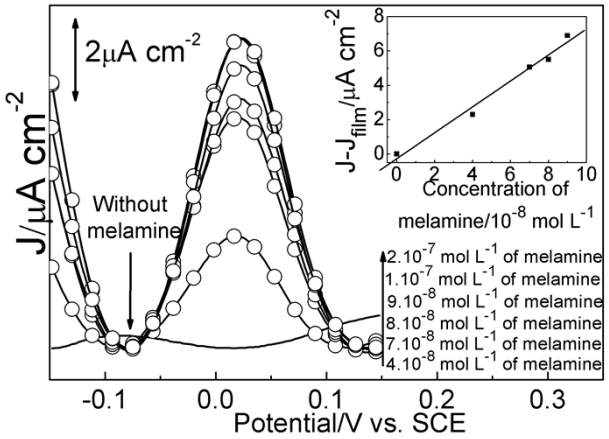

Figure S12: Differential pulse voltammograms in the anodic region for a 5-bilayers (HPW/PAH) LbL film on ITO substrate pre-coated with (PDMS/PAH) at different atrazine concentrations varying from 1.0 10^{-6} mol L^{-1} to 5.0 10^{-6} mol L^{-1}. The inset shows the anodic current density versus the atrazine concentration. The supporting electrolyte was an aqueous solution of $HClO_4$ at pH=1.0.

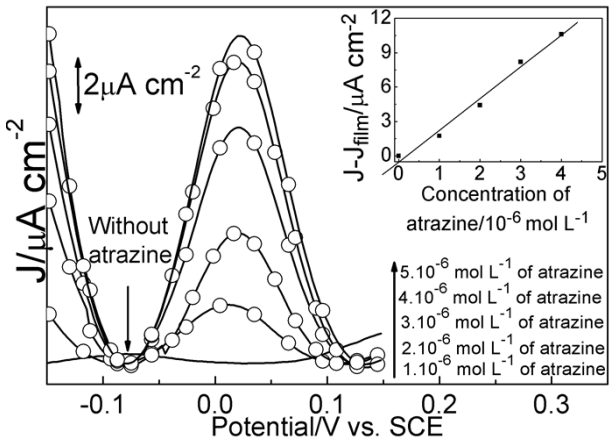

References

1) J. N. Chazalviel, U. P. Rodrigues Filho, *Thin Solid Films*, 2012, **520**, 3918.

2) J. N. Chazalviel, F. Ozanam, in *Advances in Electrochemical Science and Engineering*, ed. R. C. Alkire, D. M. Kolb, J. Lipkowski, P. N. Ross, Wiley VCH, Weinheim, 2006, pp. 199-232.

3) W. Suetaka, in *Surface Infrared and Raman Spectroscopy: methods and applications*, Plenum Press, New York, 1988, pp. 118-127.